Chemical Data Collections 15–16 (2018) 89–96

Contents lists available at ScienceDirect

Chemical Data Collections

journal homepage: www.elsevier.com/locate/cdc

Data Article

Structural elucidation and Hirshfeld surface analysis of a novel pyrazole derivative: 3-(Benzo[d][1,3]dioxol-5-yl)-1-(3-chlorophenyl)-5-(2,4-dichlorophenyl)-4,5-dihydro-1H-pyrazole

S. Naveen[a], Karthik Kumara[b], A. Dileep Kumar[c], K. Ajay Kumar[c], N.K. Lokanath[b,*]

[a] Department of Physics, School of Engineering & Technology, Jain University, Bangalore 562 112, India
[b] Department of Studies in Physics, University of Mysore, Manasagangotri, Mysuru 570 006, India
[c] Department of Chemistry, Yuvaraja's College, University of Mysore, Mysuru 570 005, India

ARTICLE INFO

Article history:
Received 1 February 2018
Revised 6 April 2018
Accepted 19 April 2018
Available online 22 April 2018

Keywords:
Pyrazoles
X-ray diffraction
Intermolecular Interactions
Hirshfeld surface
Electrostatic potential

ABSTRACT

The title compound 3-(benzo[d][1,3]dioxol-5-yl)-1-(3-chlorophenyl)-5-(2,4-dichlorophenyl)-4,5-dihydro-1*H*-pyrazole was synthesized by the reaction of (*E*)-1-(benzo[d][1,3]dioxol-5-yl)-3-(2,4-dichlorophenyl)prop–2-en-1-one and (3-chlorophenyl)hydrazine hydrochloride. The synthesized compound was characterized by ^{1}H NMR, ^{13}C NMR and mass spectral analysis and finally the structure was confirmed by single crystal X-ray diffraction studies. The compound crystallizes in the triclinic crystal system with the space group *P*−*1*. The pyrazole ring in the chiral racemate adopts an envelope conformation with the compound possessing a chiral center at C3 with *R* conformation. The molecular structure involves C—H···π and Cg···Cg interactions. Also, the crystal structure is stabilized by both inter and intra-molecular hydrogen bonds of the type C—H…Cl and C—H…N respectively which can account for the stability of the molecule. Further, Hirshfeld surface analysis employing 3D molecular surface contours and 2D fingerprint plots have been used to analyze intermolecular interactions present in the solid state of the crystal.

Specifications Table

Subject area	Organic Chemistry, Crystallography
Compounds	3-(Benzo[d][1,3]dioxol-5-yl)-1-(3-chlorophenyl)-5-(2,4-dichlorophenyl)-4,5-dihydro-1*H*-pyrazole
Data category	Synthesis, Crystallographic data and Hirshfeld surface calculations
Data acquisition format	*CIF* for crystallography
Data type	Analyzed
Procedure	The compound $C_{22}H_{15}Cl_3N_2O_2$, 3-(benzo[d][1,3]dioxol-5-yl)-1-(3-chlorophenyl)-5-(2,4-dichlorophenyl)-4,5-dihydro-1*H*-pyrazole was synthesized and single crystals suitable for X-ray diffraction studies were grown from ethanol using slow evaporation technique. Prismatic green coloured single crystal of approximate dimensions 0.37 × 0.28 × 0.23 mm was chosen for X-ray diffraction studies. X-ray intensity data were collected for different settings of φ(0° and 90°), keeping the scan width of 0.5°, exposure time of 5 s and the sample to detector distance of 45.10 mm at 293 K.
Data accessibility	CCDC 1819418

* Corresponding author.
E-mail address: lokanath@physics.uni-mysore.ac.in (N.K. Lokanath).

https://doi.org/10.1016/j.cdc.2018.04.006
2405-8300/

1. Rationale

Chalcones were regarded as useful building blocks in organic synthesis, particularly for the construction of a variety of biological important compounds [1]. Five-membered heterocyclic compounds, in particular pyrazole derivatives have been extensively studied for their versatile synthetic utilities and biological applications [2]. The synthesis and biological properties of pyrazole and its derivatives have been a very special topic in the field of organic and medicinal chemistry. Pyrazole derivatives have known to exhibit broad spectrum of pharmacological applications such as anti-inflammatory and analgesic [3], anaesthetic [4], antimicrobial and antioxidant [5], anticancer [6], antiamoebic [7]. Pyrazoles and their derivatives, with change in electron donating and withdrawing groups have the capability to modulate the activity and still remain as the scaffold of choice in bioorganic and medicinal chemistry. In this perspective, structure activity relationships play a significant role in drug synthesis. Prompted by the above literature survey results, and in continuation of our research work aiming at developing a straightforward and flexible method towards effective synthesis of novel pyrazoles [8–11], we herein report the synthesis, characterization, single crystal X-ray diffraction studies and Hirshfeld surface analysis of a new molecule 3-(benzo[d][1,3]dioxol-5-yl)-1-(3-chlorophenyl)-5-(2,4-dichlorophenyl)-4,5-dihydro-1*H*-pyrazole.

2. Procedure

2.1. Materials and methods

In a typical reaction, a solution of (E)-1-(benzo[d][1,3]dioxol-5-yl)-3-(2,4-dichlorophenyl)prop-2-en-1-one (1), and (3-chlorophenyl)hydrazine hydrochloride (2) in methyl alcohol and 4–5 drops of conc. hydrochloric acid was refluxed on a water bath for 3 h. After completion of the reaction followed by work-up procedure, the reaction yielded 3-(benzo[d][1,3]dioxol-5-yl)-1-(3-chlorophenyl)-5-(2,4-dichlorophenyl)-4,5-dihydro-1H-pyrazole (3) in 91% yield. The reaction pathway is illustrated in Fig. 1. m.p. 142–143 °C. ^{1}H NMR and ^{13}C NMR spectra were recorded on Bruker-400 MHz and Agilent-NMR 125 MHZ spectrometer, respectively in CDCl3 with TMS as an internal standard. The chemical shifts are expressed in δ ppm. Mass spectra were obtained on Mass Lynx SCN781 spectrometer TOF mode. Elemental analyses were performed on a Thermo Finnigan Flash EA 1112 CHN analyzer.

2.2. Synthesis of 3-(benzo[d][1,3]dioxol-5-yl)-1-(3-chlorophenyl)-5-(2,4-dichlorophenyl)-4,5-dihydro-1H-pyrazole, (3)

The solution of 1-(benzo[d][1,3]dioxol-5-yl)-3-(2,4-dichlorophenyl)prop-2-en-1-one (**1**) (0.01 mol) and (3-chlorophenyl)hydrazine hydrochloride (**2**) (0.01 mol) in methyl alcohol (20 mL), 3–4 drops of acetic acid were added. The mixture was refluxed on a water bath for 3–4 h. The progress of the reaction was monitored by thin layer chromatography (TLC). After completion of the reaction, the mixture was poured into ice cold water and the solid separated was filtered, washed with ice cold water to obtain the crude product. The solid obtained was crystallized from methyl alcohol by slow evaporation to obtain pale yellow rectangular shaped crystals of 3-(benzo[d][1,3]dioxol-5-yl)-1-(3-chlorophenyl)-5-(2,4-dichlorophenyl)-4,5-dihydro-1*H*-pyrazole (**3**) in 91% yield, m.p. 182 °C. **Spectral data:** δ 3.086 (dd, 1H, *J = 9.2 Hz, 13.4 Hz*, 4-Ha), 3.958 (dd, 1H, *J = 9.8 Hz, 21.6 Hz*, 4-Hb), 5.624 (dd, 1H, *J = 8.7 Hz, 18.2 Hz*, 5-H), 6.822–7.289 (m, 9H, Ar-H), 7.430 (d, 1H, Ar-H), 7.774 (s, 2H, OCH_2O). ^{13}C NMR ($CDCl_3$): δ 43.7 (1C, 4-C), 64.1 (1C, 5-C), 102.0 (1C, OCH_2O), 111.2 (1C), 113.5 (1C), 119.0 (1C), 125.2 (1C), 125.6 (1C), 126.4 (1C), 127.3 (1C), 128.5 (1C), 129.0 (1C), 129.8 (1C), 129.9 (1C), 131.5 (1C), 134.7 (1C), 135.0 (1C), 137.6 (1C), 138.4 (1C), 142.9 (1C), 145.2 (1C), 152.0 (1C, 3-C). MS (m/z) for $C_{22}H_{15}Cl_3N_2O_2$: 448.04 (M+4, 13), 446.05 (M+2, 63), 444.07 (M+, 100). Anal. Calcd. (%): C, 59.28; H, 3.39; N, 6.29; Found (%): C, 59.13; H, 3.20; N, 6.14.

2.3. X-ray diffraction studies

A prismatic green single crystal of approximate dimensions 0.37 × 0.28 × 0.23 mm of the title compound was chosen for an X-ray diffraction study. X-ray intensity data were collected for the title compound at temperature 296 K on a Bruker Proteum2 CCD diffractometer with X-ray generator operating at 45 kV and 10 mA, using CuK_α radiation of wavelength 1.54178 Å. Data were collected for 24 frames per set with different settings of φ(0° and 90°), keeping the scan width of 0.5°, exposure

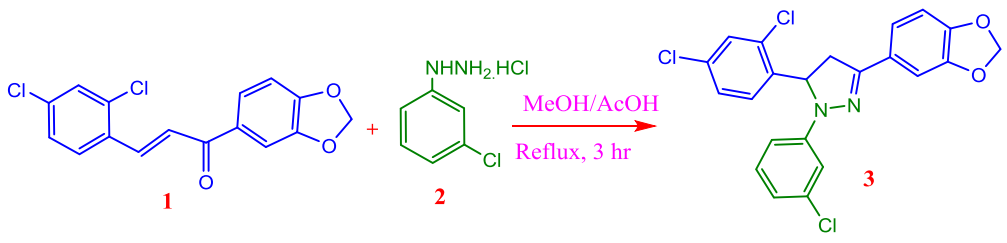

Fig. 1. Schematic diagram of the title compound.

Table 1
Crystal data and structure refinement details.

Parameter	Value
Empirical formula	$C_{22}H_{15}Cl_3N_2O_2$
Formula weight	445.71
Temperature	293 K
Wavelength	1.54178 Å
Crystal system, space group	Triclinic, $P\bar{1}$
Unit cell dimensions	$a = 7.5746(2)$ Å $b = 11.0267(3)$ Å $c = 12.5178(3)$ Å $\alpha = 100.032(2)^o$ $\beta = 101.8870(10)^o$ $\gamma = 103.415(2)^o$
Volume	967.74(4) Å^3
Z	2
Density (calculated)	1.530 Mg m^{-3}
Absorption coefficient	4.477 mm^{-1}
F_{000}	456
Crystal size	0.37 × 0.28 × 0.23 mm^3
θ range for data collection	6.22° to 64.64°
Index ranges	$-8 \le h \le 8$ $-12 \le k \le 12$ $-14 \le l \le 14$
Reflections collected	10,236
Independent reflections	3148 [$R_{int} = 0.0613$]
Absorption correction	multi-scan
Refinement method	Full matrix least-squares on F^2
Data / restraints / parameters	3461 / 0 / 201
Goodness-of-fit on F^2	1.078
Final [$I > 2\sigma(I)$]	$R1 = 0.0559$, $wR2 = 0.1650$
R indices (all data)	$R1 = 0.0710$, $wR2 = 0.1928$
Largest diff. peak and hole	0.570 and − 0.552 e Å^{-3}
CCDC Number	CCDC 1819418

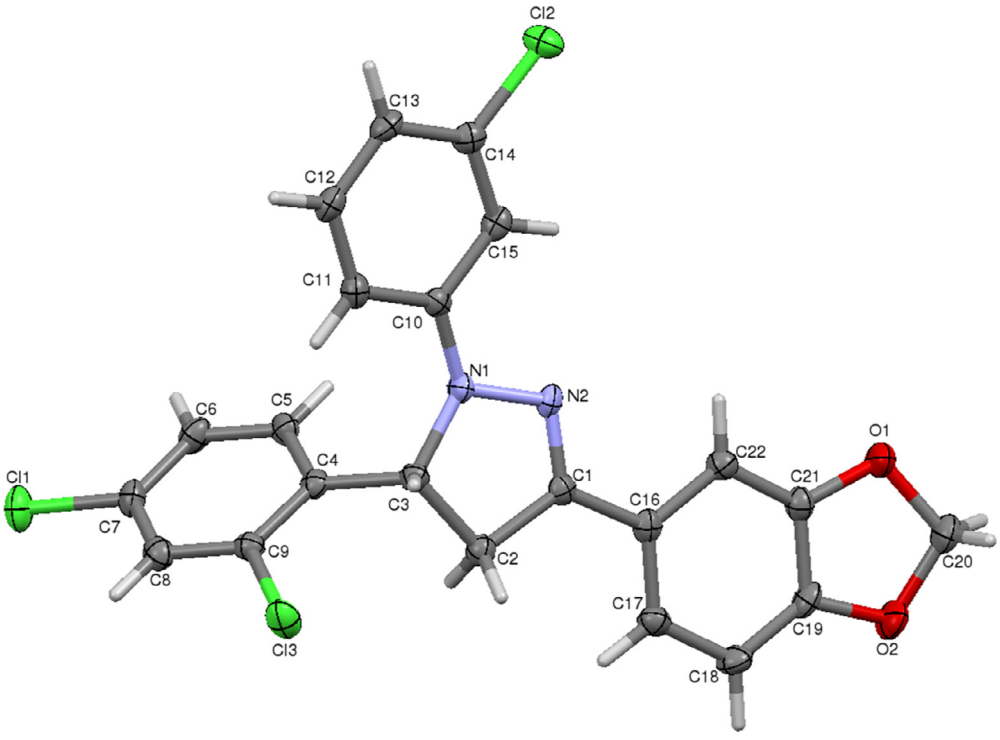

Fig. 2. ORTEP diagram of the molecule with thermal ellipsoids drawn at 50% probability.

Table 2
Bond lengths (Å).

Atoms	Length	Atoms	Length
Cl1–C7	1.739(3)	C5–C6	1.383(5)
Cl2–C14	1.747(4)	C6–C7	1.388(5)
Cl3–C9	1.746(3)	C7–C8	1.381(5)
O1–C21	1.377(4)	C8–C9	1.380(5)
O1–C20	1.425(5)	C10–C11	1.401(5)
O2–C19	1.385(4)	C10–C15	1.410(5)
O2–C20	1.446(5)	C11–C12	1.373(5)
N1–C10	1.382(5)	C12–C13	1.380(5)
N1–N2	1.393(4)	C13–C14	1.392(5)
N1–C3	1.472(4)	C14–C15	1.377(5)
N2–C1	1.287(5)	C16–C17	1.387(5)
C1–C16	1.467(5)	C16–C22	1.412(4)
C1–C2	1.508(4)	C17–C18	1.396(5)
C2–C3	1.544(5)	C18–C19	1.359(5)
C3–C4	1.518(5)	C19–C21	1.393(5)
C4–C5	1.393(5)	C21–C22	1.362(5)
C4–C9	1.397(5)		

Table 3
Selected Bond angles (°).

Atoms	Angles	Atoms	Angles
C21–O1–C20	105.4(3)	C4–C9–Cl3	119.2(3)
C19–O2–C20	104.1(3)	N1–C10–C11	121.3(3)
C10–N1–N2	119.6(3)	N1–C10–C15	120.4(3)
C10–N1–C3	124.0(3)	C11–C10–C15	118.4(3)
N2–N1–C3	112.7(3)	C12–C11–C10	120.8(3)
C1–N2–N1	108.3(3)	C11–C12–C13	121.6(3)
N2–C1–C16	121.8(3)	C12–C13–C14	117.5(3)
N2–C1–C2	114.1(3)	C15–C14–C13	122.8(3)
C16–C1–C2	124.0(3)	C15–C14–Cl2	117.8(2)
C1–C2–C3	102.1(3)	C13–C14–Cl2	119.3(3)
N1–C3–C4	112.8(3)	C14–C15–C10	118.9(3)
N1–C3–C2	101.9(2)	C17–C16–C22	120.0(3)
C4–C3–C2	112.4(3)	C17–C16–C1	119.9(3)
C5–C4–C9	117.1(3)	C22–C16–C1	120.2(3)
C5–C4–C3	121.4(3)	C16–C17–C18	122.2(3)
C9–C4–C3	121.4(3)	C19–C18–C17	116.9(3)
C6–C5–C4	121.9(3)	C18–C19–O2	128.6(3)
C5–C6–C7	118.6(3)	C18–C19–C21	121.6(3)
C8–C7–C6	121.5(3)	O2–C19–C21	109.7(3)
C8–C7–Cl1	119.3(3)	O1–C20–O2	107.5(3)
C6–C7–Cl1	119.2(3)	C22–C21–O1	128.3(3)
C9–C8–C7	118.3(3)	C22–C21–C19	122.5(3)
C8–C9–C4	122.4(3)	O1–C21–C19	109.3(3)
C8–C9–Cl3	118.3(2)	C21–C22–C16	116.9(3)

time of 5 s, the sample to detector distance of 45.10 mm. The experimental analysis reveals that the synthesized compound crystallizes in the triclinic crystal system, in $P-1$ space group with unit cell parameters $a = 7.5746(2)$ Å, $b = 11.0267(3)$ Å, $c = 12.5178(3)$ Å, $\alpha = 100.032(2)^{o}$, $\beta = 101.8870(10)^{o}$, $\gamma = 103.415(2)$ with unit cell volume, $V = 967.74(4)$ Å^3. A complete data set was processed using *SAINT PLUS* [12]. The structure was solved by direct methods and refined by full-matrix least squares method on F^2 using *SHELXS* and *SHELXL* programs [13]. All the non-hydrogen atoms were revealed in the first difference Fourier map itself. All hydrogen atoms were positioned geometrically (C–H = 0.93 Å) and refined using a riding model with $U_{iso}(H) = 1.2\ U_{eq}(C)$. After several cycles of refinement, the final difference Fourier map showed peaks of no chemical significance and the residual is saturated to 0.0559. The geometrical calculations were carried out using the program *PLATON* [14].The molecular and packing diagrams were generated using the software *MERCURY* [15]. The details of the crystal structure and data refinement are given in Table 1. The list of bond lengths, bond angles and torsion angles of the non-hydrogen atoms are given in Tables 2–4 respectively. Fig. 2 represents the *ORTEP* of the molecule with thermal ellipsoids drawn at 50% probability.

A study of torsion angles, asymmetric parameters and least squares plane reveals that the central pyrazole ring adopts a flattened envelope conformation with the atom C3 deviating 0.055(4) Å from the Cremer and Pople plane. This is confirmed by the puckering amplitude $Q = 0.088(4)$ Å and $\varphi = 152(2)^{\circ}$. Also, the dioxalane ring adopts an envelope conformation with

Table 4
Torsion angles (°).

Atoms	Angles	Atoms	Angles
C10–N1–N2–C1	166.5(3)	N1–C10–C11–C12	−177.1(3)
C3–N1–N2–C1	7.3(4)	C15–C10–C11–C12	2.0(5)
N1–N2–C1–C16	176.7(3)	C10–C11–C12–C13	−0.8(5)
N1–N2–C1–C2	−1.6(4)	C11–C12–C13–C14	−0.6(5)
N2–C1–C2–C3	−4.1(4)	C12–C13–C14–C15	0.7(5)
C16–C1–C2–C3	177.6(3)	C12–C13–C14–Cl2	−178.9(2)
C10–N1–C3–C4	71.7(4)	C13–C14–C15–C10	0.5(5)
N2–N1–C3–C4	−130.1(3)	Cl2–C14–C15–C10	−179.9(2)
C10–N1–C3–C2	−167.5(3)	N1–C10–C15–C14	177.2(3)
N2–N1–C3–C2	−9.4(3)	C11–C10–C15–C14	−1.8(5)
C1–C2–C3–N1	7.6(3)	N2–C1–C16–C17	−174.4(3)
C1–C2–C3–C4	128.6(3)	C2–C1–C16–C17	3.8(5)
N1–C3–C4–C5	21.8(4)	N2–C1–C16–C22	5.2(5)
C2–C3–C4–C5	−92.7(4)	C2–C1–C16–C22	−176.7(3)
N1–C3–C4–C9	−159.4(3)	C22–C16–C17–C18	1.4(5)
C2–C3–C4–C9	86.1(4)	C1–C16–C17–C18	−179.0(3)
C9–C4–C5–C6	0.2(5)	C16–C17–C18–C19	0.1(5)
C3–C4–C5–C6	179.1(3)	C17–C18–C19–O2	−178.6(3)
C4–C5–C6–C7	0.5(5)	C17–C18–C19–C21	−1.8(5)
C5–C6–C7–C8	−0.2(5)	C20–O2–C19–C18	−170.7(4)
C5–C6–C7–Cl1	−178.9(3)	C20–O2–C19–C21	12.2(4)
C6–C7–C8–C9	−0.7(5)	C21–O1–C20–O2	19.7(4)
Cl1–C7–C8–C9	177.9(3)	C19–O2–C20–O1	−19.6(4)
C7–C8–C9–C4	1.5(5)	C20–O1–C21–C22	168.3(4)
C7–C8–C9–Cl3	−177.9(3)	C20–O1–C21–C19	−12.2(4)
C5–C4–C9–C8	−1.2(5)	C18–C19–C21–C22	2.1(6)
C3–C4–C9–C8	179.9(3)	O2–C19–C21–C22	179.4(3)
C5–C4–C9–Cl3	178.2(3)	C18–C19–C21–O1	−177.5(3)
C3–C4–C9–Cl3	−0.7(4)	O2–C19–C21–O1	−0.2(4)
N2–N1–C10–C11	−169.8(3)	O1–C21–C22–C16	179.0(3)
C3–N1–C10–C11	−13.1(5)	C19–C21–C22–C16	−0.5(5)
N2–N1–C10–C15	11.1(5)	C17–C16–C22–C21	−1.2(5)
C3–N1–C10–C15	167.8(3)	C1–C16–C22–C21	179.3(3)

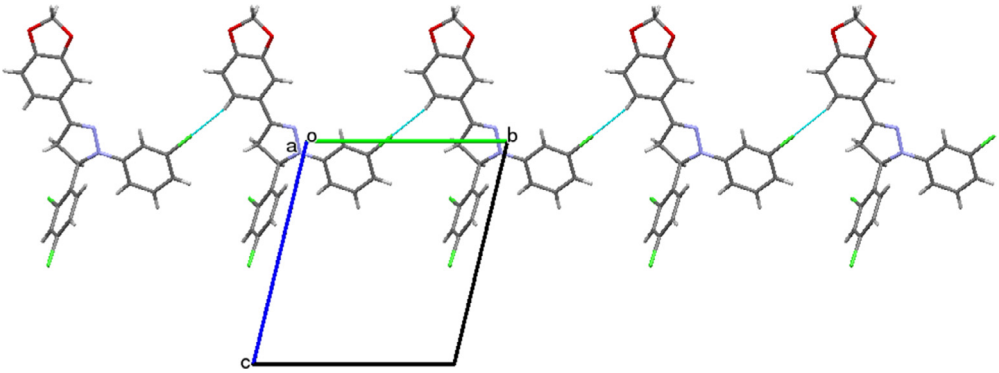

Fig. 3. Packing of the molecules when viewed down along the *a*-axis. The dotted lines represent the intermolecular C—H...Cl hydrogen bonds forming a one dimensional chain.

the atom C20 deviating 0.117(4) Å from the Cremer and Pople [16] plane. This is confirmed by the puckering amplitude $Q = 0.185(4)$ Å and $\varphi = 216.5(12)°$.

The dihedral angle between the central pyrazole ring and the chlorophenyl ring is 9.26(19) whereas that between the pyrazole ring and the fused benzo-dioxalane ring is 6.76(16)° which clearly indicates that they are nearly coplanar. Also, the dihedral angle between the pyrazole ring and the dichlorophenyl ring is 67.22(19)° whereas that between the chlorophenyl and the dichlorophenyl ring as well as dichlorophenyl and the fused benzo-dioxalane rings are 76.32(17)° and 69.15(15)° respectively. The title compound is chiral. In the arbitrarily chosen asymmetric molecule, the compound possesses a chiral center at C3 with *R* conformation. Since the compound crystallizes in a centrosymmetric spacegroup, we can surmise that the compound is a racemic mixture. The molecule exhibits C—H···π interactions; C2—H2A···*Cg*4; *Cg*4 is the centroid of the ring C10/C11/C12/C13/C14/C15) with a C—*Cg* distance of 3.462(4) Å, H···*Cg* distance of 2.67 Å, C—H···*Cg* angle of 139°, with a symmetry code 1−*x*, 2−*y*, −*z* and a halogen interaction C7—Cl1···*Cg3; Cg*3 is the centroid of the ring C4/C5/C6/C7/C8/C9)

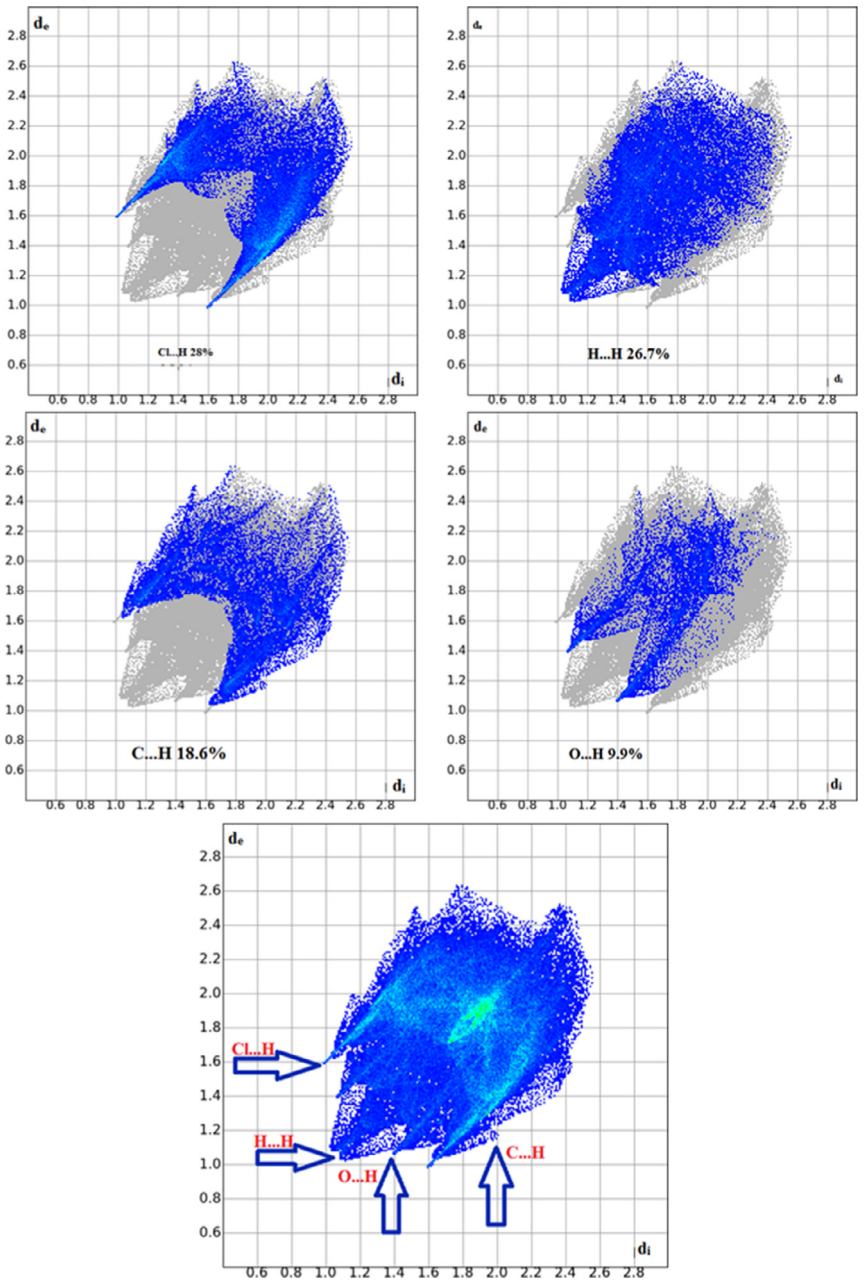

Fig. 4. Fingerprint plots and corresponding surface area of the title compound showing the individual contribution of each interaction.

with aC—*Cg* distance of 4.177(4) Å, Cl···*Cg* distance of 3.98(2) Å, C—Cl···*Cg* angle of 83.82(1)°, with a symmetry code*1*−*x*, *2*−*y*, *1*−*z*.

The structure also exhibits *Cg*···*Cg* interactions: *Cg*2···*Cg*3 (*Cg*2 is the centroid of the ring N1/N2/C1/C2/C3) with a *Cg*—*Cg* distance of 3.902(2) Å, $\alpha = 67.22(19)$, $\beta = 57.9°$, $\gamma = 81.7°$, a perpendicular distance of *Cg*2 on the ring C4/C5/C6/C7/C8/C9 = −0.5617(16) Å and symmetry code *x*, *y*, *z*, similarly, *Cg*2···*Cg*4 with a *Cg*—*Cg* distance of 3.844(2) Å, $\alpha = 9.26(19)°$, $\beta = 29.4°$, $\gamma = 20.8°$, a perpendicular distance of *Cg*2 on the ring C10/C11/C12/C13/C14/C15 = 3.5945(15) Å with a symmetry code *1*−*x*, *2*−*y*, −*z*. Further the crystal structure is stabilized by both inter and intramolecular hydrogen bonds of the type C—H···Cl and C—H…N respectively. The C17—H17…Cl2 hydrogen bond has a length of 3.623(4) Å and an angle of 164° with a symmetry code *x*, *−1 + y*,*−z* links the molecules to form a one dimensional chain when viewed down along the *a* axis (Fig. 3).

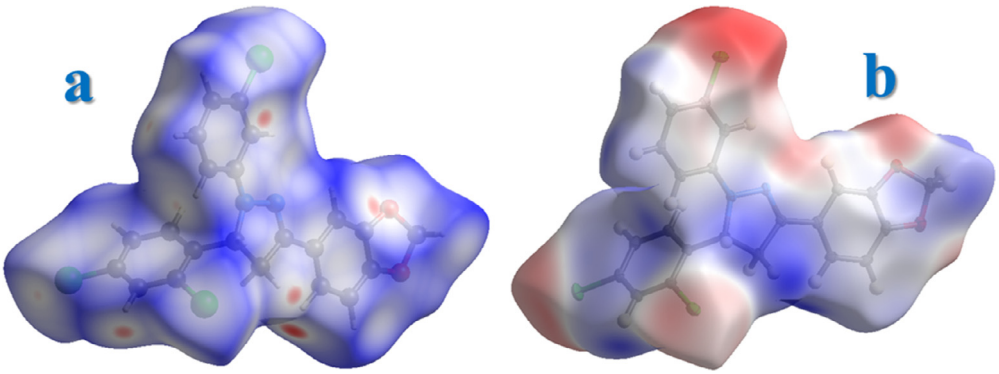

Fig. 5. **(a)** d_{norm} and **(b)** electrostatic potential mapped on Hirshfeld surface for visualizing the intermolecular contacts.

2.4. Hirshfeld surface studies

Hirshfeld surface analysis (HSA) is a unique way of graphical visualization of the intermolecular interactions of the crystal structure. HSA was carried out by uploading crystallographic information file (CIF) to the Crystal Explorer version 17 software [17]. The calculated volume inside the Hirshfeld surface is 474.99 $Å^3$ in the area of 429.40 $Å^2$ with globularity (G) 0.686 as well as asphericity (Ω) 0.149. The overall calculationswere performed with the TONTO [18] integrated with Crystal Explorer. The identification of the regions of particular importance to intermolecular interactions is obtained by mapping normalized contact distance (d_{norm}), expressed as:

$$d_{norm} = \left(d_i - r_i^{vdw}\right)/r_i^{vdw} + \left(d_e - r_e^{vdw}\right)/r_e^{vdw}$$

where r_i^{vdw} and r_e^{vdw} are the van der Waals radii of the atoms. The value of d_{norm} is negative or positive when intermolecular contacts are shorter or longer than r^{vdw}, respectively. Graphical plots of the molecular Hirshfeld surfaces mapped with d_{norm} employ the red—white–blue color scheme where red color indicates the shorter intermolecular contacts, white color shows the contacts around the r^{vdW} separation, and blue color is used to indicate the longer contact distances. Because of the symmetry between d_e and d_i in the expression for d_{norm}, where two Hirshfeld surfaces touch, both will display a red spot identical in color intensity as well as size and shape. The d_{norm} plot was mapped on Hirshfeld surface with color scale in between −0.189 au (blue) to 1.211 au (red) respectively. The color codes on the surface can be used for the analysis of the molecular contacts, such that regions with red and blue color on the d_{norm} represent the shorter and longer inter contacts while the white color indicates the contacts around the Vander Waals radii [19,20].

The expanded two dimensional fingerprint plots displayed in the range of 0.6–2.8 Å with the d_e and d_i distance scales displayed on the graph axes [21–23] (Fig. 4). Where d_i is the closest internal distance from a given point on the Hirshfeld surface and d_e is the closest external contacts. The contribution of each individual intermolecular contact to the surface can be identified through color codes on FP. If $d_i > d_e$ then this represents the dark regions on the surface which are due to interaction of hydrogen bond acceptors. Similarly, the regions with $d_e > d_i$ value are due to the hydrogen bond acceptors. The white color indicates no occurrence, blue indicates some occurrence, green and red indicating more frequent occurrence of any given (d_i, d_e) pair. Fig. 4 revealed that the Cl…H contacts has maximum contribution whereas the H…H, C…H and O···H contacts also contribute to the total area of the Hirshfeld surface.

The C–H…π and π…π interactions are evidently given in fingerprint plots. The inter contact distances obtained from HSA are in good agreement with experimental crystallographic data. The two of the spikes with points at d_e and d_i in the fingerprint plot illustrate that the value of ($d_e + d_i = 1 + 1.60$) is 2.60 Å for Cl…H interactions in the donor and acceptor regions of the Fingerprint plots. These molecular interactions are highlighted on the Hirshfeld surface using conventional mapping of d_{norm} and electrostatic potential (Fig. 5). The shape index is most sensitive to very subtle changes in surface shape, the red patches on them represent by concave regions indicating atoms of the π-stacked molecule above them and the blue triangles represent by convex regions indicating the ring atoms of the molecule inside the surfaces.

The red triangles on the shape index mapping are referred to the C—H…π interactions and the information conveyed by shape index is in good agreement with the 2D fingerprint plot. The curvedness is a measure of the shape of the surface area of the molecule. The flat areas of the surface correspond to low values of curvedness, while sharp curvature areas correspond to high values of curvedness and usually tend to divide the surface into patches indicating the interactions between neighboring molecules. The large flat region which is delineated by a blue outline refers to the $\pi \cdots \pi$ stacking interactions (Fig. 6).

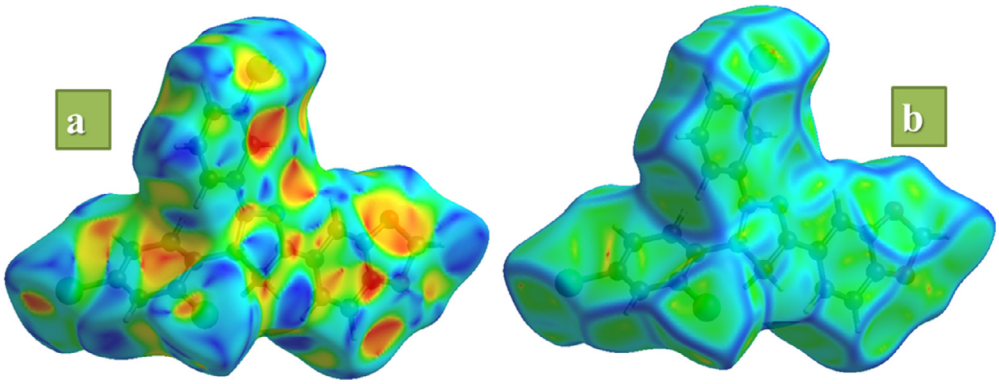

Fig. 6. **(a)** Shape index and **(b)** Curvedness mapped on Hirshfeld surface for visualizing the intermolecular contacts.

3. Conclusions

The title compound $C_{22}H_{15}Cl_3N_2O_2$ has been synthesized and the single crystals were grown by the slow evaporation method using methanol as a solvent. The compound was characterized using the NMR and mass spectrum. The molecular structure of the compound was confirmed by the single crystal X-ray diffraction studies. The pyrazole ring in the chiral racemate adopts an envelope conformation with the compound possessing a chiral center at C3 with *R* conformation. The molecular structure involves C—H···π and Cg···Cg interactions. Also, the crystal structure is stabilized by both inter and intra-molecular hydrogen bonds of the type C—H…Cl and C—H…N respectively which can account for the stability of the molecule. Further, Hirshfeld surface analysis employing 3D molecular surface contours and 2D fingerprint plots have been used to analyze intermolecular interactions present in the solid state of the crystal.

Acknowledgments

The authors are thankful to the Institution of Excellence, Vijnana Bhavana, University of Mysore, Mysuru, for providing the X-ray intensity data and the National Facility and Department of Studies in Physics, University of Mysore, Mysuru, for providing the computational facility.

References

[1] M. Baumann, I.R. Baxendale., Beilstein J. Org. Chem. 9 (1) (2013) 2265–2319.
[2] K. Ajay Kumar, M. Govindaraju, Int. J. ChemTech Res. 8 (1) (2015) 313–322.
[3] M. Amir, H. Kumar, S.A. Khan, Bioorg. Med. Chem. Lett. 18 (2008) 918–922.
[4] B. Shivarama Holla, M. Mahalinga, B. Poojary, A. Mithun, Eur. J. Med. Chem. 15 (1980) 567–570.
[5] R. Nagamallu, B. Srinivasan, M.B. Ningappa, K. Ajay Kumar, Bioorg. Med. Chem. Lett. 26 (2016) 690–694.
[6] G. Vasanth Kumar, M. Govindaraju, N. Renuka, G. Pavithra, B.N. Mylarappa, K.Ajay Kumar, Int. J. Pharm. Sci. Res. 3 (12) (2012) 4801–4806.
[7] M. Abid, A. Azam, Bioorg. Med. Chem. Lett. 16 (2006) 2812–2816.
[8] D.M. Lokeshwari, A. Dileep Kumar, S. Bharath, S. Naveen, N.K. Lokanath, K. Ajay Kumar, Bioorg. Med. Chem. Lett. 27 (2017) 3806–3811.
[9] M.G. Prabhudeva, M. Prabhuswamy, A. Dileep Kumar, N.K. Lokanath, S. Naveen, K. Ajay Kumar, Chem. Data Coll. 9–10 (2017) 80–88.
[10] A. Dileep Kumar, Karthik Kumara, S. Naveen, N.K. Lokanath, K. Ajay Kumar, Chem. Data Coll. 9–10 (2017) 89–97.
[11] K. Kumara, S. Naveen., L.D. Mahadevaswamy, K.Ajay Kumar, N.K. Lokanath, Chem. Data Coll. 9 (2017) 251–262.
[12] Bruker, APEX2, SAINT-Plus and SADABS, Bruker AXS Inc., Madison, Wisconsin, USA, 2004.
[13] G.M. Sheldrick, Acta Cryst. C71 (2015) 3–8.
[14] A.L. Spek, Acta Cryst. A46 (1990) c34–c34.
[15] C.F. Macrae, I.J. Bruno, J.A. Chisholm, P.R. Edgington, P. McCabe, E. Pidcock, L.M. Rodriguez, R. Taylor, J. van de Streek, P.A. Wood, J. Appl. Cryst. 41 (2008) 466–470.
[16] D.T. Cremer, J.A. Pople, J. Am. Chem. Soc. 97 (6) (1975) 1354–1358.
[17] J. Bernstein, R.E. Davis, L. Shimoni, N-L. Chang, Int. Ed. 34 (1995) 1555–1573.
[18] D. Jayatilaka, D.J. Grimwood, A. Lee, A. Lemay, A.J. Russell, The University of Western Australia, Nedlands, 2005.
[19] K. Kumara, K.P. Harish, S. Naveen, H.C. Tandon, K.N. Mohana, N.K. Lokanath, Chem. Data Coll. 11–12 (2017) 40–58.
[20] K. Kumara, M. Jyothi, S. Naveen, Zabiulla, S.A. Khanum, N.K. Lokanath, Chem. Data Coll. 9–10 (2017) 152–163.
[21] S.K. Seth, Cryst. Eng. Comm. 15 (2013) 1772–1781.
[22] S.K. Seth, J. Mol. Struct. 1064 (2014) 70–75.
[23] S. Naveen, G. Sudha, E. Suresha, N.K. Lokanath, P.A. Suchetan, Z. Kristallogr. 232 (11) (2017) 767–780.